

50-83 850

I-12626

UCID--19946

DR-2008-7

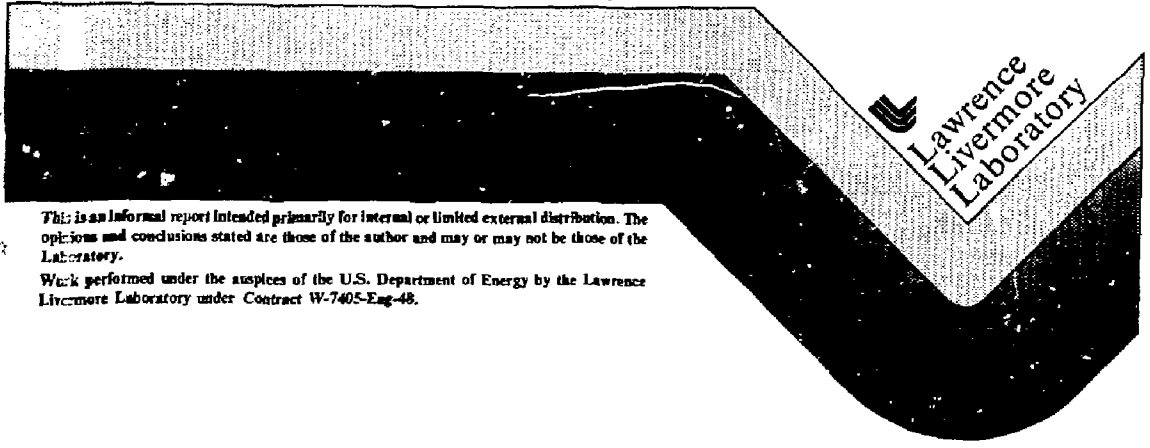
UCID--19946

DE84 004703

S-20 Photocathode Research Activity -- Part I

Francoise Gex
Observatoire de Paris, Paris, France
Tony Huen and Ralph Kalibjian
Lawrence Livermore National Laboratory
Livermore, California, U.S.A.

November 22, 1983



Lawrence
Livermore
Laboratory

This is an informal report intended primarily for internal or limited external distribution. The opinions and conclusions stated are those of the author and may or may not be those of the Laboratory.
Work performed under the auspices of the U.S. Department of Energy by the Lawrence Livermore Laboratory under Contract W-7405-Eng-48.

MASTER

DISTRIBUTION OF THIS DOCUMENT IS UNLIMITED

S-20 PHOTOCATHODE RESEARCH ACTIVITY -- PART I*

Francoise Gex
Observatoire de Paris-DOPTO, 77, Av. Denfert Rochereau,
75014, Paris, France,

Tony Huen and Ralph Kalibjian
Lawrence Livermore National Laboratory,
P.O. Box 5508, Livermore, California 94550

1. INTRODUCTION

The goal of this activity has been to develop and implement S-20 photocathode processing techniques at Lawrence Livermore National Laboratory (LLNL) in order to study the physical properties of the photocathode films. The present work, Part I, is the initial phase of a planned activity in understanding cathode fabrication techniques and the optical/electrical characterization of these films. Part II (to be published) will deal with the evaluation of the physical properties of these films.

2. EXPERIMENTAL DEVICES

The apparatus used in the photocathode research activity is shown in Figure 1, which consists of the photocathode processing vacuum station and the required power sources/instrumentation panels.

2.1 Vacuum Chamber

The vacuum system (5 l/s Varian pump) used for processing the photocathodes is shown in Figure 2. This system can attain an ultimate pressure better than 1×10^{-6} Torr. The design of the test envelope (7052 Corning glass) is shown schematically in Figure 3. An important feature of the glass chamber is the three metal gasket vacuum flanges that allow the system to be easily demounted for cleaning the chamber after each use. Multi-lead headers are connected to two of the flanges and the third flange connects to the pump via a cold trap.

DISCLAIMER

This report was prepared as an account of work sponsored by an agency of the United States Government. Neither the United States Government nor any agency thereof, nor any of their employees, makes any warranty, express or implied, or assumes any legal liability or responsibility for the accuracy, completeness, or usefulness of any information, apparatus, product, or process disclosed, or represents that its use would not infringe privately owned rights. Reference herein to any specific commercial product, process, or service by trade name, trademark, manufacturer, or otherwise does not necessarily constitute or imply its endorsement, recommendation, or favoring by the United States Government or any agency thereof. The views and opinions of authors expressed herein do not necessarily state or reflect those of the United States Government or any agency thereof.

MASTER

DISTRIBUTION

tip

2.2 Sources Mounting

An eight pin header is used for evaporating the source metals as shown in Figure 4. The antimony source is a bead of pure solid antimony melted on a platinum coated molybdenum wire. Just before mounting the bead, it is degassed in a neutral gas atmosphere with a 2 A current. A nickel shield around the bead limits the evaporated film to the target area and thus prevents the deposition of the antimony on the inside walls of the chamber, which otherwise would obscure light and photoemission current measurements.

The alkali sources, potassium, sodium, and cesium are dispenser channels manufactured by SAES Getters Company. Such channels are commonly used in commercial photocathode production. These metal dispensers consist of an alkali metal chromate and a reducing agent such as Zr. By initiating the reducing reaction at high temperatures, the alkali metal may be generated in situ.

These channels are heated electrically under external control as shown in the electrical diagram of Figure 5. Very accurate control of the quantity of alkali metal released is achieved simply by controlling the amount of current in the dispenser. The current is adjusted by a rheostat and read on an ammeter. The practical current range for these dispensers is from 5 to 7.5 A depending on the deposition rate required.

2.3 The Substrate

The substrate consists of a 20-pin, 2 mm thick 7052 Corning glass plate which is ground and polished flat on one side. The pins are spaced linearly 2 mm apart as shown in Figure 6. The plate is fabricated by ultrasonically drilling holes, inserting 0.5 mm Kovar pins, and fusing the metal pins to the glass at 800°C in a graphite block.

After polishing and cleaning the flat surface, twenty rectangular-shaped metallic bars (centered on each pin) are evaporated in vacuum through an appropriate mask.

Finally the twenty pins of the substrate are spot welded to the twenty pins of the header and the electrical contacts checked with an ohmmeter before assembling the substrate into the vacuum chamber.

2.4 Monitoring and Measurement Equipment

During the processing, the antimony evaporation is controlled by monitoring the optical transparency of the film, and the alkali metal evaporation is monitored by the photoemission current. The substrate is positioned diagonally between two line-of-sight windows as shown in Figure 7. One window is used to illuminate the substrate by means of a quartz-iodine lamp that is placed inside the oven. A photomultiplier receiving the light coming through the substrate at the second window measures the transmitted light. For measuring the photoemission current the antimony bead and its shield are connected to the ground and used as an anode. A Keithly model 410 microammeter is inserted in series with this anode. The negative pole of a power supply (-300 V) is connected to the twenty shorted pins of the substrate. Depending on the lamp's position either the photoemission in reflection or transmission can be measured.

After the processing, a small single pass I.S.A. Insta-monochromator is used for the light source (instead of the quartz-iodine lamp) for measuring the spectral response of the photocathode. The calibration at each wavelength of the incident light is performed with a calibrated R.C.A. photomultiplier with a S-20 photocathode.

3. PHOTOCATHODE PROCESSING

3.1 Preparation of the Vacuum Chamber

Component parts intended for assembly into high-vacuum devices must always be scrupulously cleaned as well as on subsequent exposures to atmosphere in order to remove alkali hydroxides formed on exposure to air. The cleaning for the glass envelope, the two headers and the substrate is accomplished as follows:

1. Rinse thoroughly in warm tap water
2. Rinse in boiling water with V.W.R. Labtone detergent
3. Rinse thoroughly in tap water
4. Rinse in distilled water
5. Dry in warm air blast
6. Rinse in pure ethyl alcohol
7. Dry in warm air blast.

The antimony bead and the alkali channels are spot welded on the header and the envelope sealed at the flanges with copper gaskets. At a pressure of 3×10^{-6} Torr in the initial pump-down and before baking the system, the alkali channels are degassed for ten minutes for the following temperature (and corresponding current in the channels):

Cs : 520°C , (6.2 A)

K : 580°C . (1.6 A)

Na : 700°C , (5.6 A)

Alkali metals are extremely reactive with oxygen, water vapor, and some other materials (2); thus it becomes important to achieve proper conditioning. Since the vapor pressure of antimony at 350°C is about 10^{-6} Torr, higher temperature than 300°C is prohibited in the baking. This low temperature is compensated by a longer baking time for a minimum of twelve hours with a 5 l/s vacuum pump. After the bake-out cycle, the alkali channels are once again degassed as before.

3.2 Processing Schedule for the S-1} (Sb-Cs) Photocathode

Two different methods have been used:

3.2.1 The one described by A. Sommer (1) is commonly used in industrial fabrication. The processing consists of two steps:

- a) Antimony is first evaporated at room temperature. The thickness of the film is controlled by observing the optical transmission. Optimum thickness is obtained when the transmission of white light is reduced to 80% of its original value.

The envelope is then heated to a temperature between 130-150°C. When this temperature is reached, the power source for the Cs channel is switched-on to slowly evolve Cs from the channel while the photoemission is monitored. The cesium source is switched-off just after the peak sensitivity has been attained. This results in a subsequent drop in sensitivity that can be reactivated by baking the tube until the peak reading has been restored.

- b) The photoemission tends to increase as the envelope cools to room temperature.

3.2.2 The second method has been developed at the Paris Observatory. The photocathodes realized by this process are more stable and can easily be transferred to another vacuum chamber without any change in sensitivity. The processing is performed at a lower temperature between 80°C and room temperature.

- a) First a small amount of cesium is evolved until a weak photoelectric current appears due to cesium photoemission.

Sb is then slowly evaporated in order to complete the stoichiometry of Cs₃Sb. The reaction is controlled by monitoring the photoelectric current. As soon as Sb is evaporated, the photoemission increases very fast up to a maximum. Sb evaporation is stopped when the peak current maximum is reached.

- b) As in the so called S-20 "yo-yo cycle", Cs and Sb are then added in small amounts in alternating steps until the maximum photoemission is reached.
- c) In order to insure an excess of cesium, the cesium is the last deposition in the yo-yo cycle. Then as in the previous method the baking of the envelope is continued until the peak reading has been restored and then cooled to room temperature.

3.3 Processing Schedules for the S-20 (Cs-Na-K-Sb) Photocathode

Two different methods will be described:

3.3.1 The more conventional method has been developed by Dr. A. Sommer who discovered the tri-alkali photocathode. On our request Dr. A. Sommer spent one day as a consultant to LLNL to explain to us his processing technique. His suggestions have been very helpful. The processing schedule is as follows:

- a) Sb is evaporated as in the S-11 processing method.
- b) A K_3Sb cathode is formed by exposing the Sb film to K vapor at about $160^{\circ}C$.
- c) The K_3Sb is exposed to Na vapor at about $220^{\circ}C$. During this step the K in K_3Sb is gradually displaced by Na. The introduction of Na is continued until a sharp drop in photosensitivity is recorded, thus indicating the presence of excess Na.
- d) To restore the correct Na:K stoichiometry ratio, small amounts of Sb and K are added in alternating steps, at about $160^{\circ}C$, until peak sensitivity is obtained. Depending on the amount of excess Na introduced in step (c), as many as 50 Sb-K alternating steps may be required. Figure 8 shows the recording of the change of the photoemission current during the so called yo-yo cycle.

e) Sb and Cs are then added in alternating steps similar to the K-Sb process described before. The Cs-Sb process is also performed at about 160°C and it is continued until peak sensitivity is attained.

3.3.2 Numerous modifications of these processes exist. Recently a new processing technique has been developed in which there is no need for the deposition of the initial layer of antimony. This new method gives very high sensitivity as well.

In this new technique described by G. Ghosh and B. P. Varma (2) potassium is deposited on the substrate heated to 180°C . When a very small photosensitivity is registered with the potassium film on the substrate, the antimony metal is evaporated in small controlled amounts. The sensitivity begins to rise and the antimony supply is switched off after a peak sensitivity has been reached. For the formation of Na_2KSb , the K_3Sb layer is activated with sodium at 200°C until the photosensitivity reaches a peak and begins to decrease.

Simultaneous evaporation of potassium and antimony is then started at a temperature of 185°C . The evaporation rates are carefully controlled to maintain a steady increase until it reaches the maximum value. The preparation of a Na_2KSb (Cs) cathode involves a further step. After the Na_2KSb cathode is formed, the temperature is reduced to 160°C when the cesium activation is started. When the sensitivity begins to droop from the maximum (as obtained by cesium activation), Sb evaporation at a controlled rate is then started. This simultaneous evaporation increases the sensitivity to high values. This is followed by a slight excess Cs deposition before cooling the envelope to room temperature.

Figure 9 gives the typical spectral response (with lime glass windows) for the tri-alkali (S-20) photocathode as compared with the cesium antimonide (S-11) cathode.

4. EXPERIMENTS AND RESULTS

Ten S-20 photocathodes and four S-11 photocathodes have been processed during the eight months of experimental work. We will describe each experiment in a chronological order and give the results for each.

Before starting an S-20 photocathode processing schedule, it has proven beneficial to test the structure of the processing chamber with an S-11 photocathode which is simpler to produce since only one alkali metal is involved.

Two Cs₃Sb photocathode processing experiments allowed us to adjust the evaporation rate with a current of 2 A in the antimony bead and a current of 5.5 A in the Cs channel. After the first experiment, we redesigned the nickel shield surrounding the antimony bead in order to optimize the uniformity of the Sb deposition. After having obtained a respectable quantum efficiency for the S-11 photocathode, we were then ready to start the first experiment with the S-20 photocathode.

4.1 S-20 Photocathodes, No. 1-2-3

The substrate was a bare glass substrate with a silver painted electrode for the electrical contact.

The first goal of these three experiments was to optimize the S-20 processing schedule (taking into account the configuration of the glass chamber) and to set-up the monitoring instrumentation. We used the method described in 3.3.2 for these first three evaporations and carried out the measurement of the spectral sensitivity in reflection and transmission. Figure 10 shows the spectral response curves for cathodes No. 2 and 3.

In a well defined geometrical configuration the volume resistivity ρ is calculated from the formula:

$$\rho = \frac{Rde}{L}$$

where R is the film resistance between the contacts A-B, L is the film length, d is the film width, and e is the film thickness.

Different methods are used for determining the thickness of multi-alkali metal photocathodes (3-4). An approximate value of the thickness can be determined by comparing the curve shapes of the measured optical reflectance as a function of the wavelength. Measurements made on cathode No. 3 give an estimated thickness of 40 nm. This is based upon the ratio α of the photosensitivity in the reflection mode to the photosensitivity in the transmission mode as determined for an irradiated wavelength λ for a given film thickness e (3). For $\lambda = 450 \text{ nm}$ and $\lambda = 525 \text{ nm}$, the corresponding ratio is $\alpha_{450} \approx 0.8$ and $\alpha_{525} \approx 0.6$.

The 40 nm thickness is generally too small for a good response tri-alkali photocathode. During the processing of the photocathode No. 3, the power supply sources for the channels were not sufficiently isolated from one another, thus causing vapor evolution from undesired channels; consequently, the cathode was not adequately processed in the yo-yo cycle, which produced a thin layer cathode.

4.2 S-20 Photocathodes, No. 4-5-6-7

A substrate has been patterned with ten silver bars, each bar centered onto a kovar pin. The geometry of the pattern is shown in Figure 11, each rectangular bar is 10 mm long and 0.3 mm wide. The processing schedule used for these two photocathodes is similar to the one described in 3.3.1.

4.2.1 Cathode No. 4

Optical Measurements

The spectral response curves in reflection and transmission modes are shown in Figure 11. The comparison of these two curves indicates that the film layer is thicker than those in No. 2 and No. 3. The absorption

of the layer explains the drop in sensitivity in the blue region of the spectrum in the transmission mode. In the red region of the spectrum, because of the thicker film, the sensitivity at 750 nm is appreciably higher than the sensitivity of No. 2 and 3 at the same wavelength. This observation is confirmed by the optical reflection curve which gives an evaluation of 90 nm thick in agreement with $\alpha_{436} = 1.8$ and $\alpha_{578} = 1$.

Electrical Measurements

I-V characteristics are measured between pairs of adjacent bars for both polarity. For the five pairs of silver bars, the I-V curves are quite linear, thus indicating a good ohmic contact between the photocathode and the silver bar. The resistance R deduced from these experiments for $L = .07$ cm, $d = 1$ cm, $e = 90$ nm is $2.8 \text{ K } \Omega < R < 4 \text{ K } \Omega$ or the resistivity is $.36 \text{ } \Omega \cdot \text{cm} \cdot \rho < .5 \text{ } \Omega \cdot \text{cm}$.

For only one pair of silver bars, the I.V curve was recorded at 100°C .

4.2.2 Cathode No. 5-6-7

These three photocathodes are similar to cathode No. 4, using the same substrate and the same processing schedule.

The sensitivity for the three photocathodes were very poor because of the following reasons:

- a) A vacuum leak occurred in the 20 pin header. The leak was sealed with Delta-Bond, and subsequently the chamber was used for processing photocathodes, but with a bake-out temperature limited to 230°C .
- b) It appeared that the silver-painted electrodes were behaving like a getter for the Cs; thus, the Cs source appeared to be rapidly depleted.

The results for these three cathodes, No. 5, 6, and 7 are summarized below:

No	Sensitivity for $\lambda = 550 \text{ nm}$	Photocathode Film Resistivity
5	5.5 mA	330 Ω - cm
6	9	50
7	2	rectifying contact

4.3 S-20 Photocathode, No. 8

This photocathode was deposited on a new substrate with seven different evaporated metals (aluminum, nickel, palladium, platinum, gold, Chromium and silver). The metal bar patterns are shown in Figure 12. Every other bar in the pattern is an aluminum bar.

Because of the twenty opaque bar pattern, it was difficult to evaluate the film thickness with the optical reflection method. Consequently, we decided to use the processing technique described in 3.3.1. By evaporating first (of the same amount) the photocathode maintains almost the same thickness approximately 90 nm for our experiments.

Optical Measurements

Optical measurements were made on the photocathode on a spot smaller than the width of the bar. For each bar the uniformity of the cathode is checked on different points on the bar. At the same time, the reflected light from each bar is also measured. Table 1 presents these measurements. The variance between the measurements on the eight aluminum bars was about 10% thus indicating a fairly uniform photocathode over the entire substrate area.

With respect to Table 1, the following observations are made:

- a) The photoemission is different from one metal substrate to another. This difference can be explained partially upon the variation of the reflected light from the different metal substrates.

- b) For the aluminum substrate, the photoemission is higher in the red region of the spectrum.
- c) The most surprising result is the very poor sensitivity of the cathode on the silver and the palladium substrates. The case of the silver may be explained with the very low reflectance. In fact, before the evaporation of the antimony film, we observed the lack of reflection on the silver substrate. The silver should have been superficially oxidized before the substrate was assembled in the vacuum chamber. There is no easy explanation for the palladium substrate; the reflectance is almost the same as that of the aluminum. However, if an intermetallic compound has been formed (5), this may possibly affect the reflectance characteristics at the palladium substrate.

Electrical Measurements

I-V curves have been measured between the metal substrate pins, either between two pins in contact with the same metal, or one pin connected to an aluminum bar and the other one connected to a different metal substrate. Figure 13 shows that all of the I-V curves are straight lines with almost the same slope regardless of the type of metal substrate. We conclude ohmic contacts have been made with a bulk photocathode resistance of $27 \text{ K}\Omega < R < 38 \text{ K}\Omega$, or a resistivity of $2 \Omega\text{-cm} < \rho < 3 \Omega\text{-cm}$ for the S-20 photocathode.

4.4 S-20 Photocathode, No. 9

The same substrate as in photocathode No. 8 has been used. After cleaning the substrate, the electrical continuity for each metal bar and pin was checked on an oscilloscope. Subsequently, a $0.4 \mu\text{m}$ thick SiO_2 layer was evaporated on the entire face of the 20-pin substrate. An aluminum ring is then evaporated to the peripheral edge of the substrate.

Optical Measurements

The same measurements as in 4.3 have been performed and are presented in Table 2:

- a) The percentage of reflected light is very low; optical interference occurs between the two thin layers of SiO_2 and the photocathode.
- b) The photoemission in reflection is almost the same for all the metals for $\lambda < 650$ nm. In particular, the sensitivities on the silver and the palladium substrates are the same but different from the other metal substrates. It should be noted that the silver strip under the SiO_2 film is partially oxidized. These results on the silver and the palladium substrates confirm the hypotheses of a compound being formed between the silver (or silver oxide) and the S-20 photocathode; the same condition is assumed for the palladium.

Electrical Measurements

The I-V characteristics between two consecutive pins are presented in Figure 14. These curves are almost linear except for three pairs of pins. The slope is nevertheless 200 times greater than without the SiO_2 layer. This linearity implies a "leaky" SiO_2 film over the metal substrates. The I-V characteristics between the cathode contact and the different metal pads confirm the leakiness of the SiO_2 ; only one of these characteristics appears to be a rectifying contact. A backplate photoemission modulation experiment was carried out on this isolated metal strip: a light spot is focussed on the metal strip and a modulated voltage of less than 3 V is applied on the corresponding pin. No significant variation of the photoemission has been observed.

4.5 S-11 Photocathode, No. 1 and 2

The principal objective of these two experiments was to compare the optical and electrical characteristics with those of the S-20 photocathode.

4.5.1 No. 1

The substrate consists of seven different metal bars evaporated with the same configuration as shown in Figure 12. The processing for the photocathode is described in 3.2.2 starting with the vaporization of a small amount of cesium.

The photoemission measurements in the reflection made for the different metals are summarized in Table 3.

- a) The photosensitivity is almost the same for the aluminum, chromium, nickel, platinum and silver substrates. Unlike the S-20 photocathode, the silver does not appear to have affected the sensitivity (caution was exercised to minimize silver oxidation).
- b) The photoemission on the platinum substrate is lower by a factor of 2.
- c) It is well known (6) that cesium vapor reacts with gold to form a semiconducting compound. The formation of this compound possibly explains the reduced photoemission sensitivity on the gold substrate.

Figure 15 shows the I-V characteristics record between two pins. None of these characteristics are linear, contrary to the S-20 photocathode observations. The extrapolated resistance from these curves is $R=200 \text{ K } \Omega$.

4.5.2 No. 2

The aim of this experiment was to determine if there is a correlation between the shape of the I-V characteristics and the processing technique. Perhaps the cesium reacts with the metal during the very first evaporation (forming an intermetallic compound) which could explain the non-ohmic contacts.

We used a substrate with twenty aluminum bars. The photocathode processing was the one described in 3.2.7 with the initial evaporation of the antimony layer.

The I-V characteristics of the S-11 cathode had the same shape and the same resistance values as in 4.5.1.

4.6. Photocathode S-20 No. 10

In this experiment we attempted to configure a MOSFET structure. The twenty metal bars are aluminum. Then a 400 nm thick SiO_2 layer is evaporated over each odd metal bar to form the insulated gate as shown in Figure 16. Caution in the cleaning and the deposition has been taken to minimize leakage in the SiO_2 film.

The S-20 photocathode is evaporated with the "Sommer" processing technique.

Optical Measurements

The photosensitivity was measured with a small spot focussed on the bare aluminum bar and on the SiO_2 covered aluminum bar. The results are presented in Table 4.

Electrical Measurements

Figure 17 shows the I-V characteristics between the even numbered pins are linear and the two odd numbered pins are not linear.

The slope of the straight lines give:

$$350 \text{ K } \Omega < R < 460 \text{ K } \Omega$$

$$\text{and } 13 \text{ } \Omega\text{-cm} < \rho < 17 \text{ } \Omega\text{-cm}$$

Backplate photoemission modulation (similar to 4.4) has been performed. Some significant change in the I-V characteristics is observed (see Figure 18) in the photoemission.

5. Conclusions

S-20 photocathode processing techniques have been developed for film research purposes at Livermore. The LLNL processing station has proven to be reliable in the production of stable films with quick fabrication turn-around time; also, it has provided an apparatus that is readily accessible in performing basic electrical and optical measurements on these films. This report has shown the system capability as well as some characteristics of these films. The photocathode film characteristics are being evaluated and will be used for developing physical models for energy band-bending effects at the photocathode-glass interface. These results will be reported in a subsequent report.

5. Acknowledgment

This work was performed at the Lawrence Livermore National Laboratory. The author wishes to acknowledge Verlyn Healy for his technical aid. To Lamar Coleman for Y-Division support, to Lloyd Multhauf for L-Division support, and to Dave Goosman of B-Division.

References

1. A. Sommer, "Photoemission Materials", J. Wiley (1968).
2. Ghosh D. Varma, JAP, 49, 4549 (1978).
3. V. E. KonDrashov, et. al., Bulletin of the Academy of Sciences, 28, 1349 (1964).
4. Dolizy, Philips Technical Review, 40, 19 (1982).
5. Kiemast and Verma, Zeitschrift fner Inorganische und Allegemeine Chemie, 310, 143 (1967).
6. M. Hirashima and M. Asano, Photoelectronic Image Devices, (Eds. McGee, et. al.), Vol. 22A, p. 643, Academic Press (1965).

Doc. #3287L/0246A



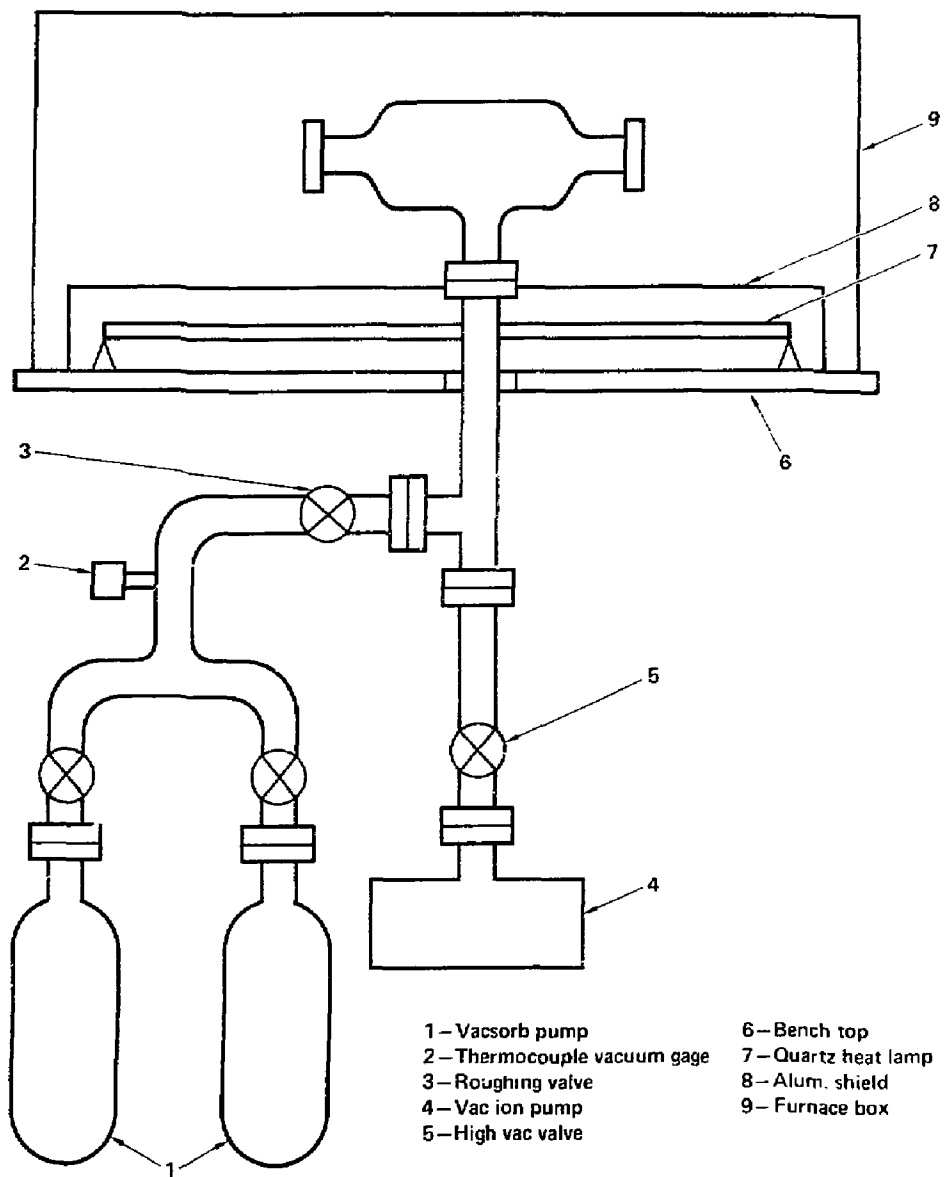


Fig. 2

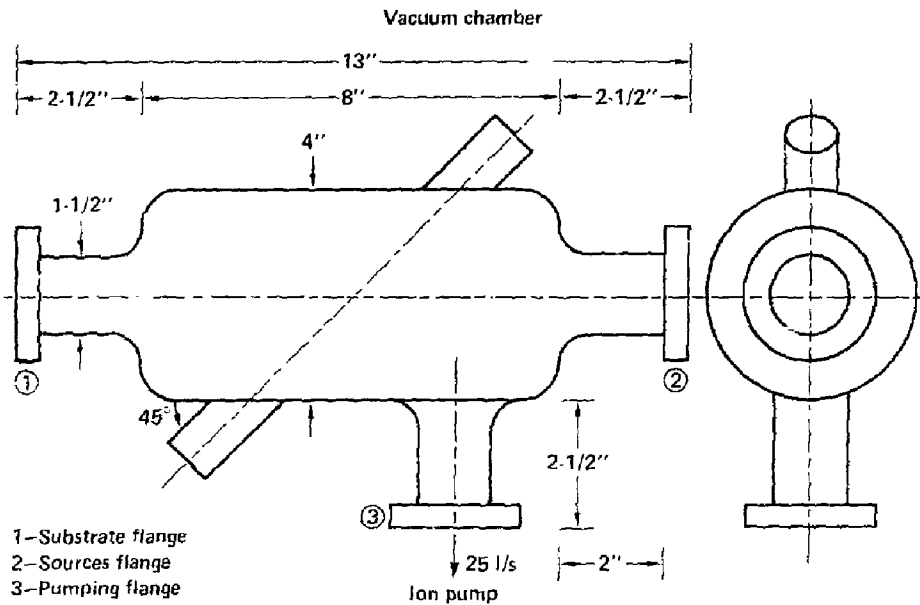
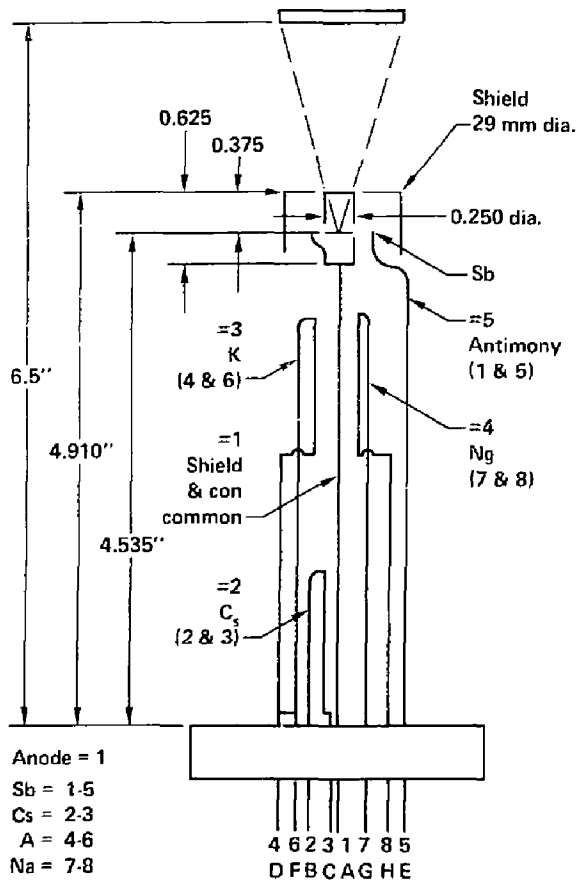


Fig. 3



First—just Sb and Cs
 Second—Sb, Cs, Na and K

Fig. 4

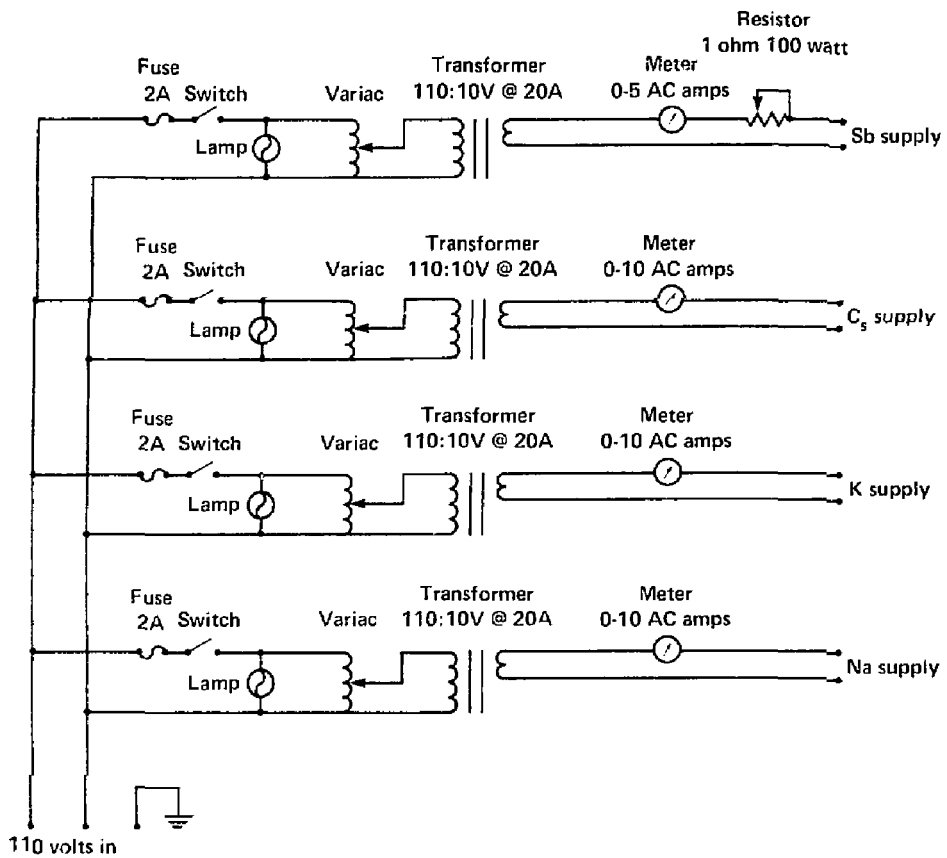


Fig. 5

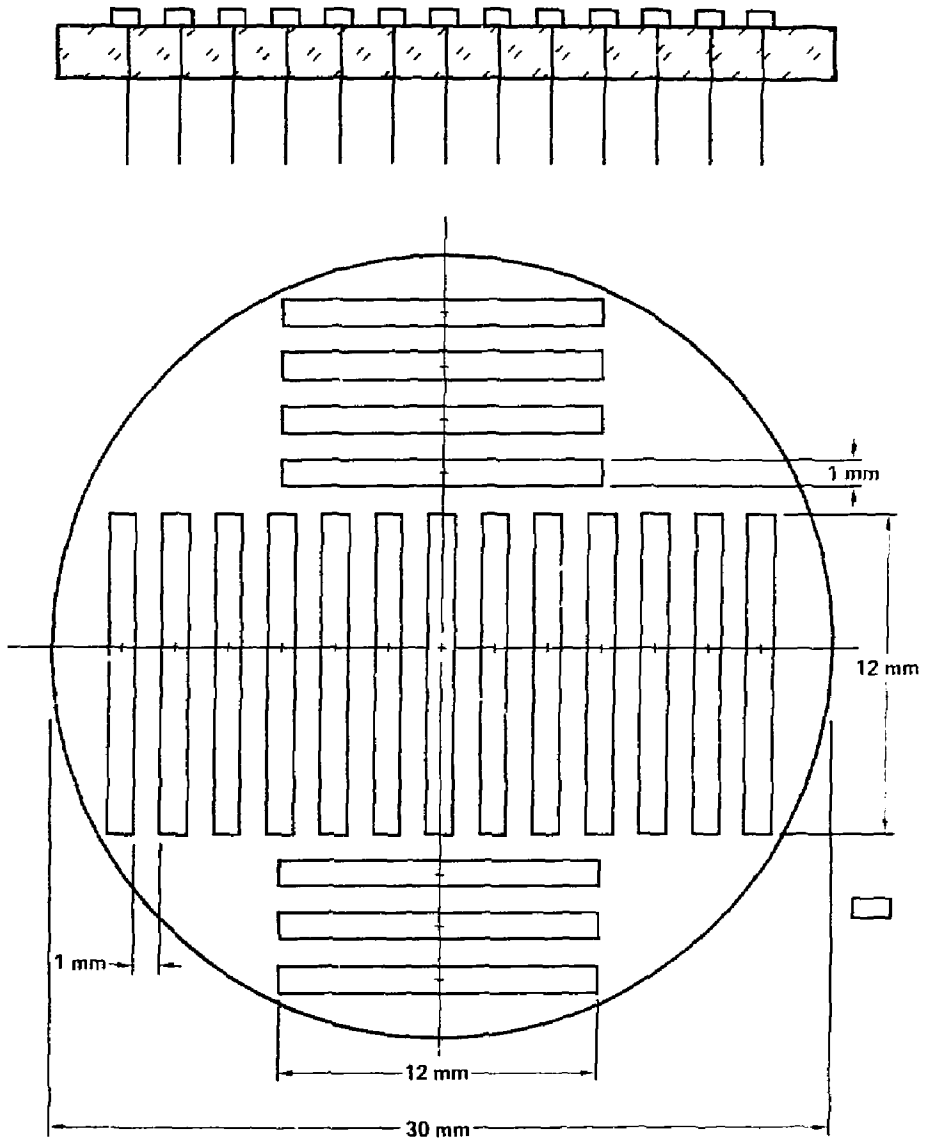
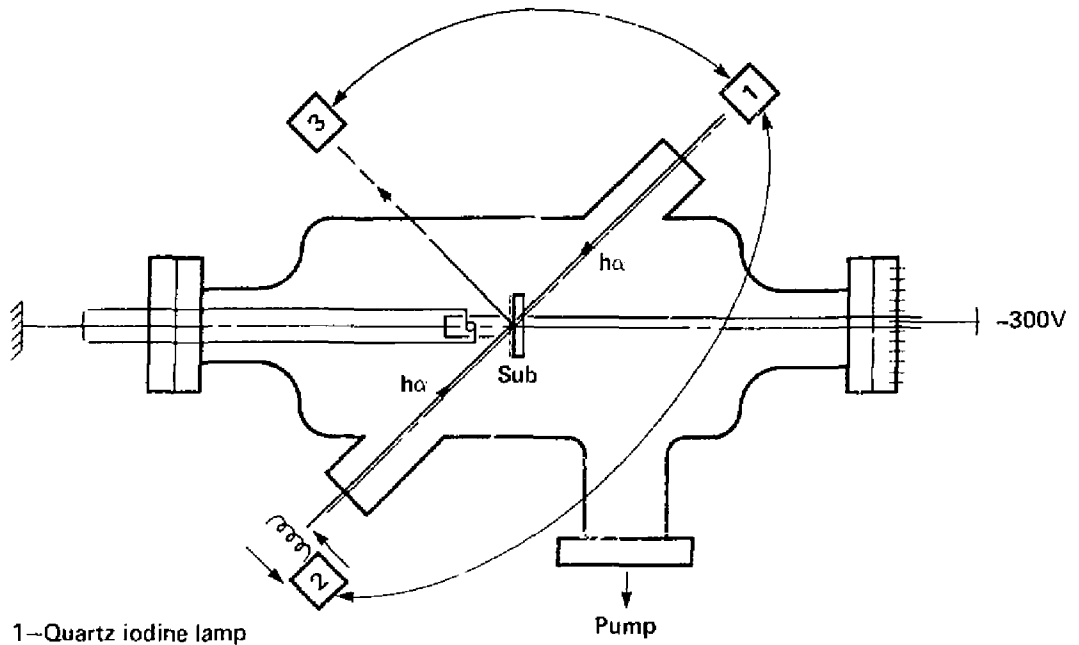


Fig. 6



- 1—Quartz iodine lamp
- 2—Monochromator ISA
- 3—R.C.A. photo-multiplier for reflection measurement

Fig. 7

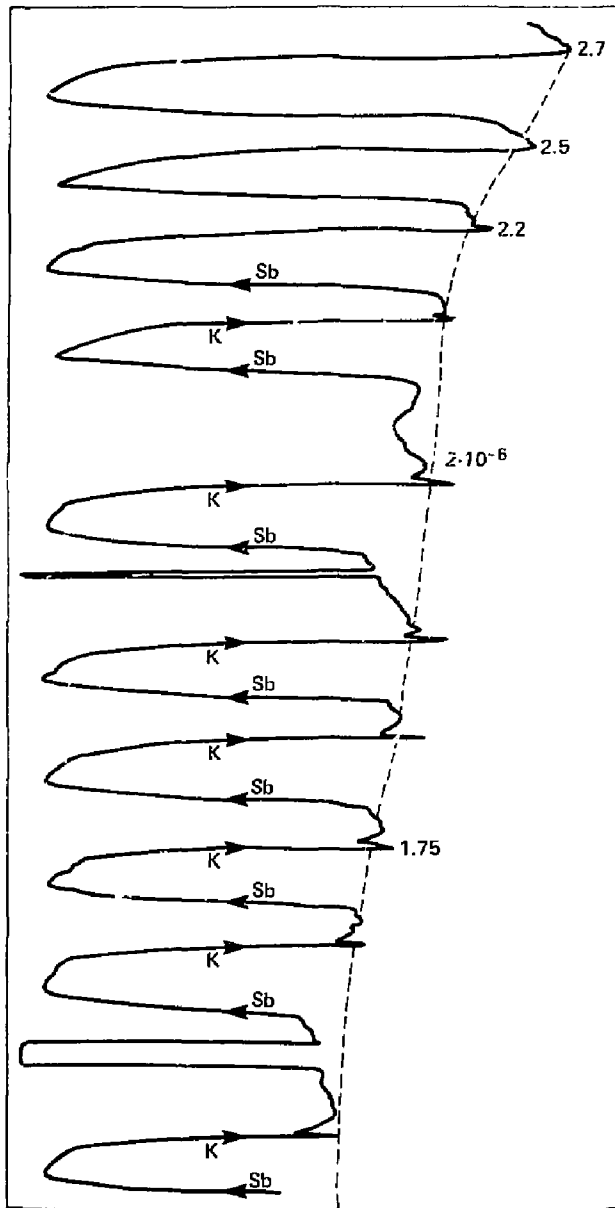


Fig. 8

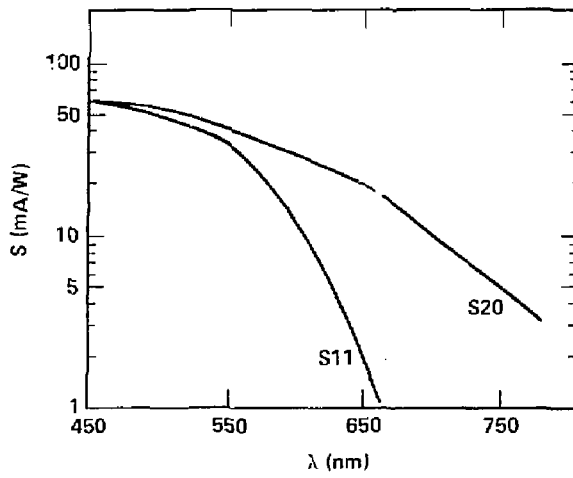


Fig. 9

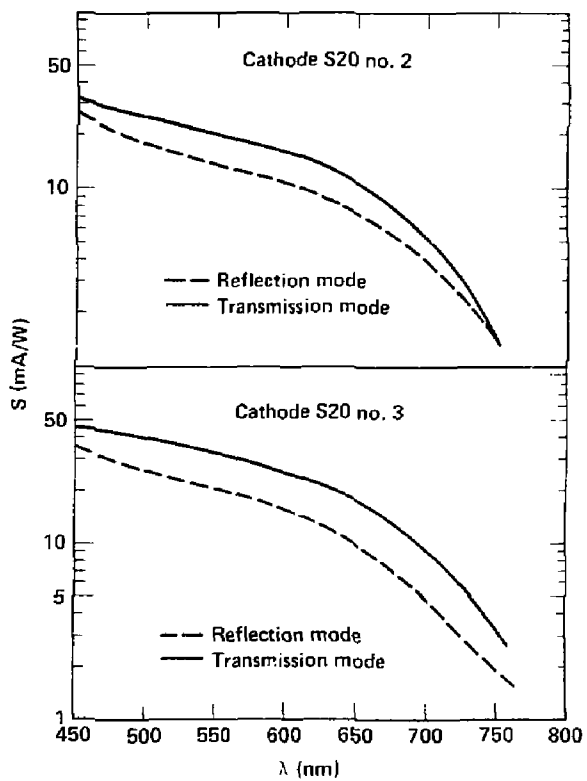


Fig. 10

Cathode S20 no. 4

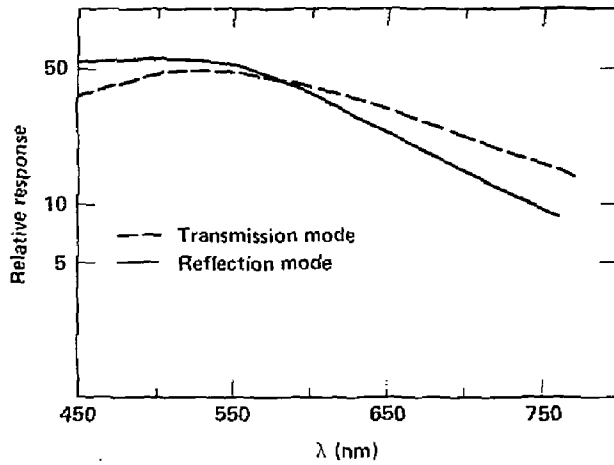
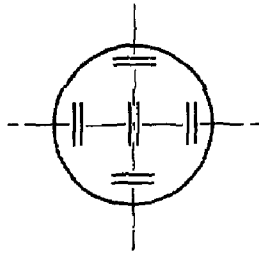


Fig. 11

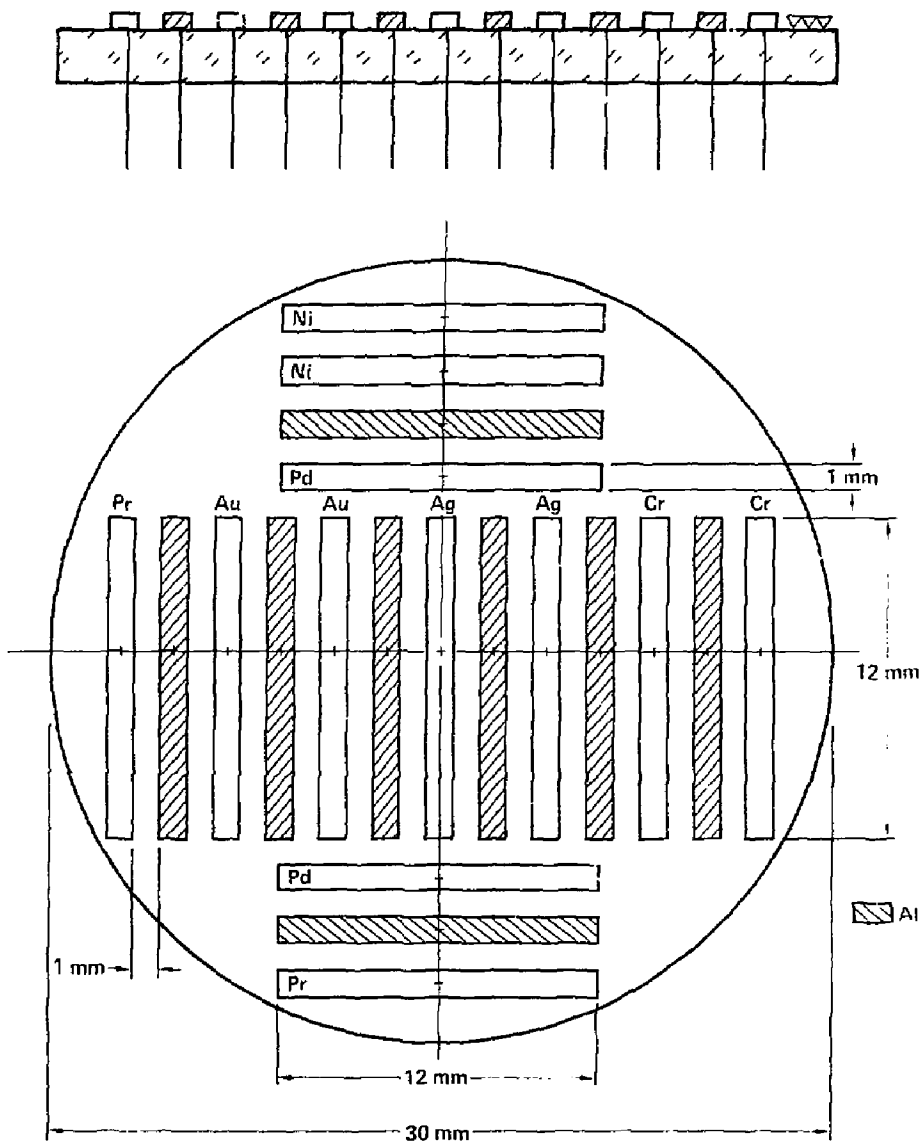


Fig. 12

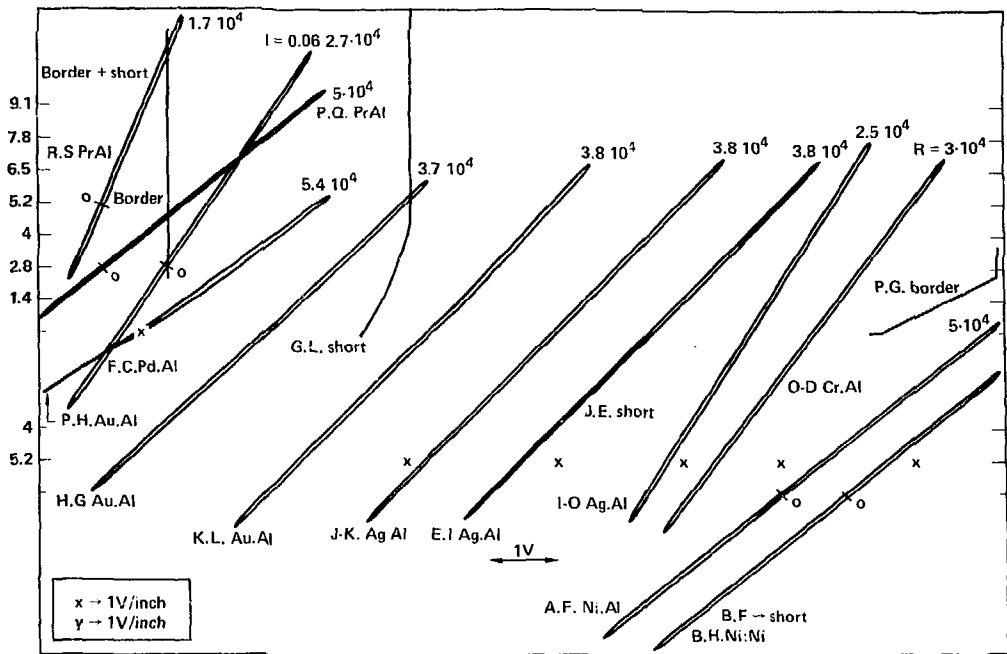


Fig. 13. $I(V)$ measured curves, with x - y recorder scale sensitivity as shown. Ammeter full scale set to 10×10^{-5} amp, Run no. 8.

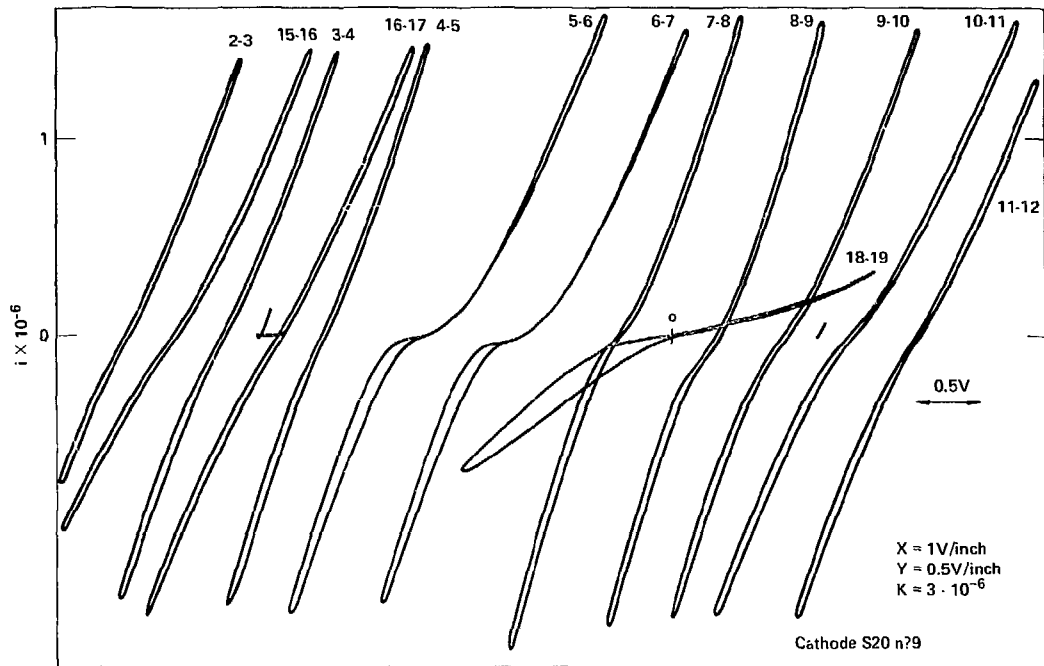


Fig. 14. $i(V)$ measurement of Run no. 9. Ammeter set at 3×10^{-6} amp full scale.

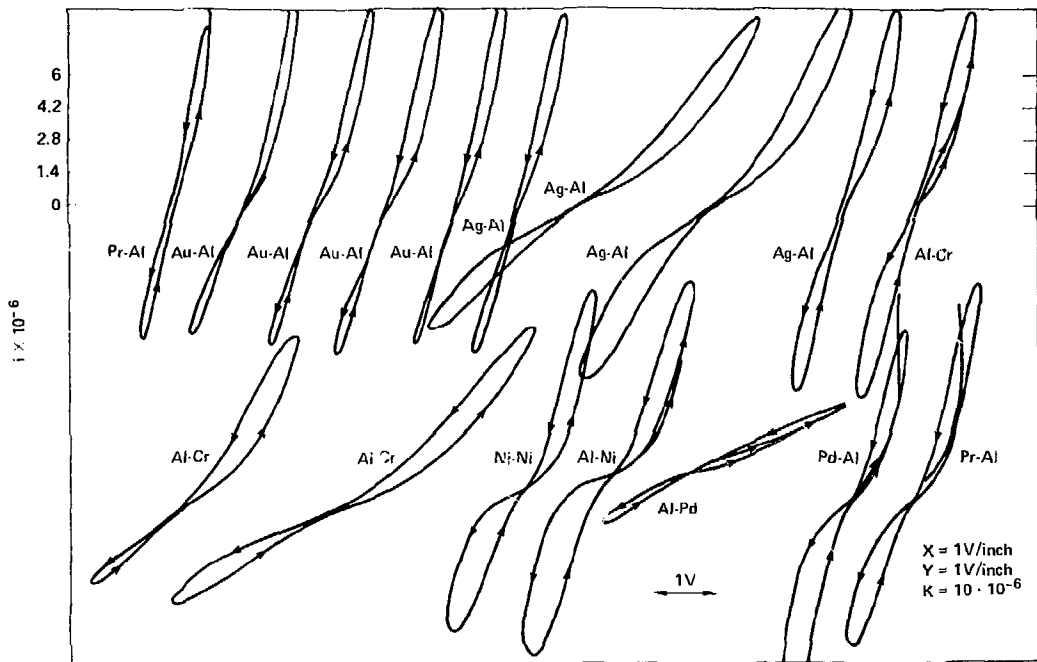


Fig. 15. I(V) measurement of S11 photocathode run.

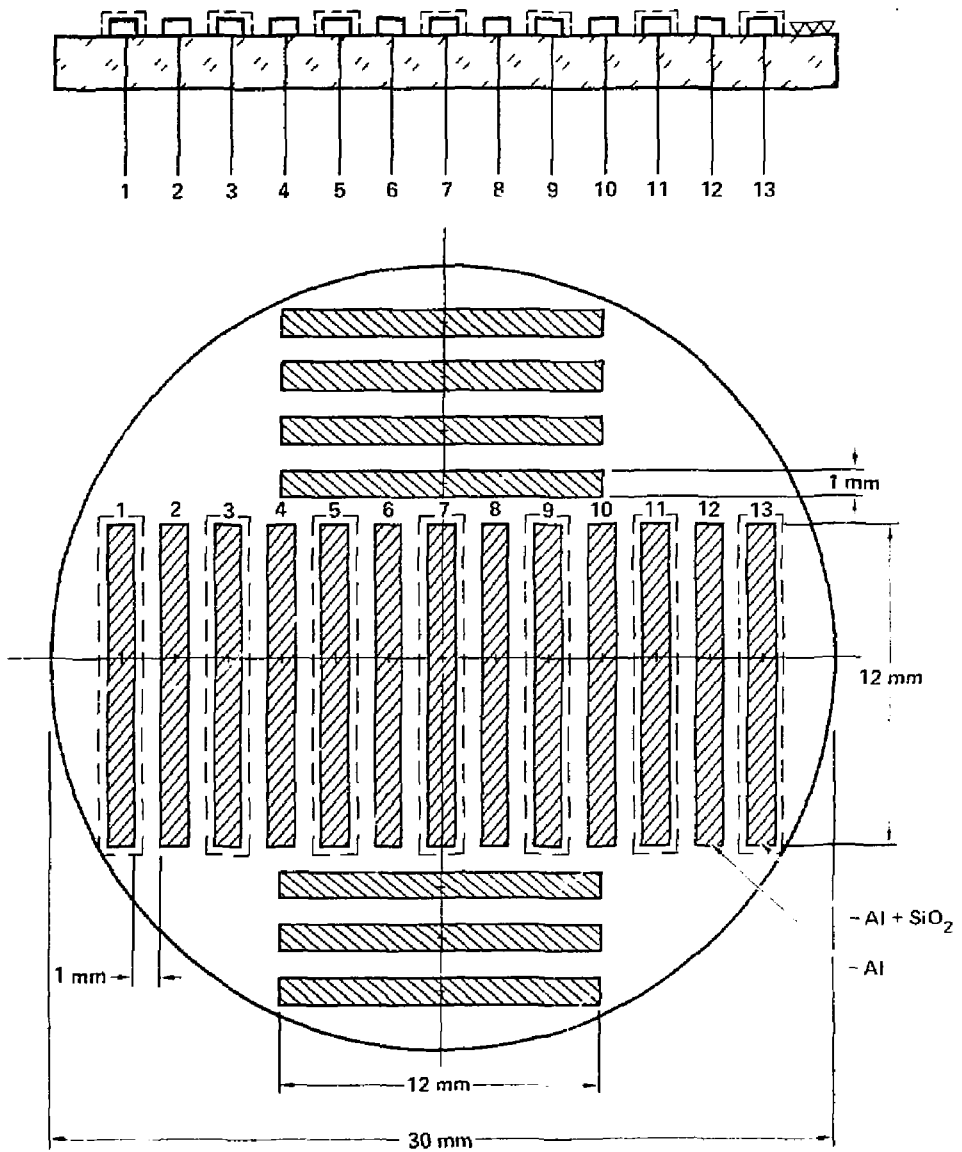


Fig. 16

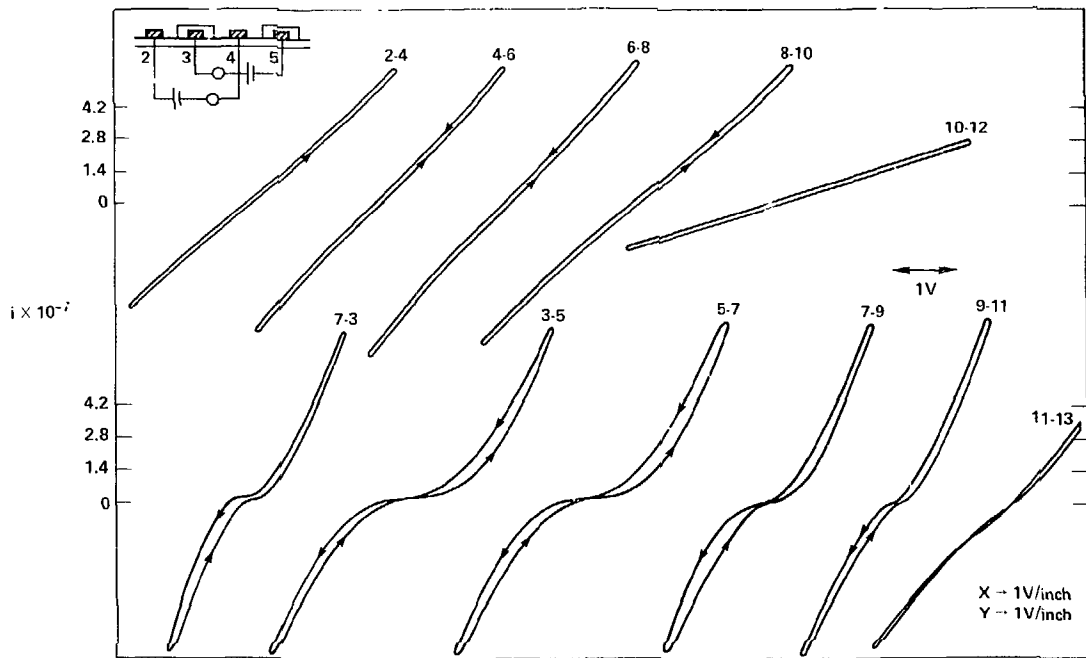


Fig. 17. $I(V)$ measurement of S20 photocathode, Run no. 10.

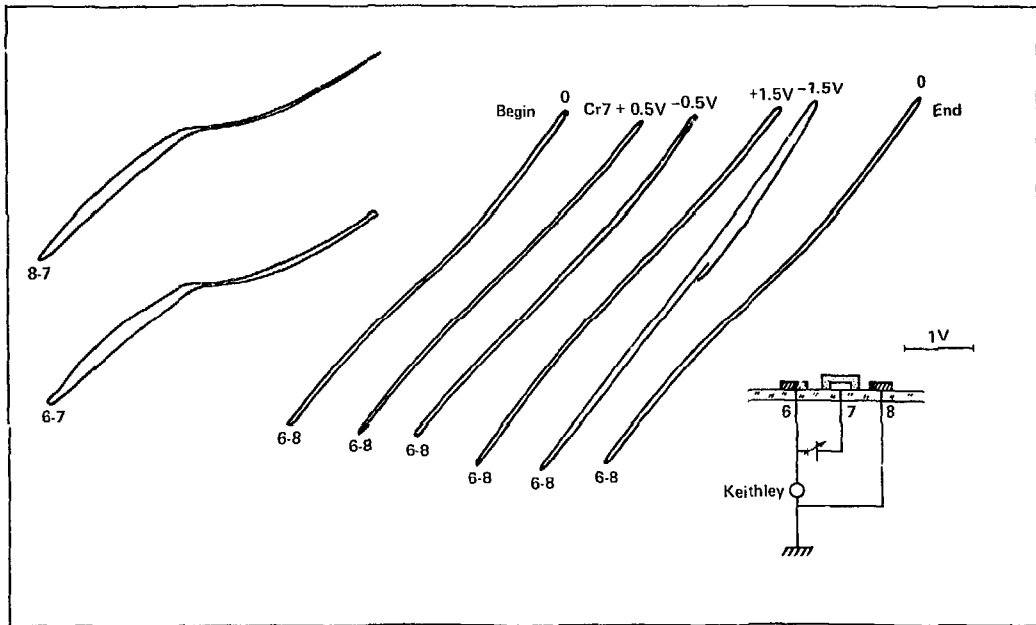


Fig. 18. $I(V)$ measurement of S20 photocathode, Run no. 10.

Table 1

λ_{nm}	Glass		Al		Au		Ni		Pr		Cr		Ag		Pd	
	Δ mA/W	R %	Δ mA/W	R %	Δ mA/W	R %	Δ mA/W	R %	Δ mA/W	R %	Δ mA/W	R %	Δ mA/W	R %	Δ mA/W	R %
450	56	23	57	24	54	26	50	19	48	27	41	29	20	8	19	25
500	37	28	47	29	36	29	37	22	37	28	37	27	14	8	12	30
550	24	32	41	29	23	41	30	21	31	28	33	26	11	9	8	34
600	16	37	37	27	18.3	43	23	18	24	26	26	22	9	10	7	38
650	9	40	22	21	14	43	14	16	15	21	16	17	6	10	3	41
700	4	50	14	16	7	49	6	16	6	19	6	15	3	10	1.5	52
750	2.5		6		4		3		3		3		2		0.9	

Table 2

λ nm	Glass		Al		Au		Ni		Cr		Ag		Pd	
	Δ mA	R %	Δ mA	R %	Δ mA	R %	Δ mA	R %	Δ mA	R %	Δ mA	R %	Δ mA	R %
450	64	1.6	68	3	60	2.9	52	2.6	61	3.6	60	3.3	71	3.1
500	38	3.8	53	5.2	41	6.2	33	5	39	6.2	44	5.6	38	7
550	24	4.8	29	8.7	36	6.4	26	4	33	4.8	32	6.7	34	5.5
600	16	4.6	24	7.2	27	6	14	5.8	18	6.8	23	6.6	20	6.7
650	9	3.5	21	5.3	13	7.3	6	5.8	9	5.8	14	5.2	8	7.6
700	4	2.5	10	2.8	7	4.2	3	3.4	4.5	3.6	6.6	2.8	4	4.2

Table 3

λ nm	Glass Δ mA/W	Al Δ mA/W	Cr Δ mA/W	Ni Δ mA/W	Pr Δ mA/W	Ag Δ mA/W	Pd Δ mA/W	Au Δ mA/W
400	43	47	44	38	41	47	19	18
450	30	35	30	30	32	32	16	13
500	29	32	29	25	27	27	13	11
550	16	17	15	13	14	14	7	5.7
600	3	4	3	2.5	3	3	1.6	1.2

Table 1

λ_{nm}	Al Δ_{main}	Al + SiO ₂ Δ_{main}
450	37	28
500	30	23
550	23	16
600	20	12
650	14	8
700	64	4